ASIAN JOURNAL OF CIVIL ENGINEERING (BUILDING AND HOUSING) VOL. 5, NOS 3-4 (2004)
PAGES 191-207

PLASTIC BUCKLING OF CYLINDRICAL SHELLS WITH CUTOUTS

E. Poursaeidi[1], G.H. Rahimi[1] and A.H. Vafai*[2]
[1] Department of Mechanical Engineering, Tarbiat Modarres University, Tehran, Iran
[2]Department of Civil Engineering, Sharif University of Technology, Tehran, Iran

ABSTRACT

The plastic behavior of an elastoplastic cylindrical shell with circular and rectangular cutouts under bending moment loads was investigated numerically and experimentally.

A testing device (pure bending measurement) was designed and made to perform experiments on bending moment tests. The ratio of diameter to thickness of the stainless steel 304 specimens was 40.4 and the ratio of length to diameter was 7.94. The shape of the cutout on the shell was circular or rectangular. The tested specimens were categorized into five dissimilar groups. The effect of size, position and numbers of the cutout on the plastic moment is discussed.

In order to investigate the strain distribution around of cutout, nine strain gauges were mounted in the longitudinal and circumferential directions on two specimens with different type of cutout.

To investigate the accuracy of analytical and experimental results, numerical analysis considering the behavior of elastoplastic material were performed and good agreement was obtained between them.

The strength of bending moment of cylindrical shells was decreased with increasing of sizes of cutout and it was increased with changing the location of the cutout from compression side to tension side. The effect of the number of cutouts (increasing from 1 to 3 (axisymmetrical)) on bending strength of tubes is negligible.

Keywords: bending buckling; cylindrical shell; cutout; FEM; experimental

1. INTRODUCTION

Cutouts are necessary either for access or for the passage of piping, ventilation ducts, uptakes, and electrical systems in cylindrical shells. A hole can be found in a missile skin, aircraft fuselage, a ship hatch, boilers and submersible pressure hulls, amongst other numerous situations. During their service life, these structures are subjected to loading of various types. In the past investigations of isotropic cylindrical shells under pure bending in the elastic range, Brazier [1] investigated the thin circular tube under pure bending and

* E-mail address of the corresponding author: vafai@sharif.edu

pointed out that the limit moment is directly related to the ovalization of the tube cross-section. Seide and Weingarten [2] used a modified Donnell equation and the Galerkin method to evaluate the maximum elastic bending buckling stress and found that it was equal to the critical compressive stress of an elastic shell under axial compression.

Circular cylindrical shells under pure bending in the plastic range were also investigated. Sherman [3] tested the bending buckling of cantilever and simple beam type of circular tubes with a ratio of diameter to thickness in the range 18–102. Reddy [4] observed the presence of wave-like ripples on the compression side of bent tubes before collapse occurred in experiments on steel and aluminum specimens. Tugcu and Schroeder [5] used a rigid-plastic material model with linear hardening for plastic buckling of pipes exposed to external couples. Gellin [6] analyzed the plastic bending buckling of infinitely long cylindrical shells. Bushnell [7] used a modified version of the BOSOR5 computer program to assess the bending buckling of straight and curved pipes. Kyriakides and Ju [8] and Ju and Kyriakides [9] investigated the instability of an aluminum cylindrical shell under pure bending with ratio of diameter to thickness in the range 19.5–60.5 and ratio of length to diameter in the range 18.1–30.1; they also observed the presence of wave-like ripples on the compression side of the bent tubes before collapse. Corona and Kyriakides [10] found that the mode of collapse was correlated with the curvature of the cylindrical shell.

Cyclic inelastic bending of tubes and the corresponding buckling problems were also reported [11–12]. When a cutout exists on a circular cylindrical shell, buckling usually occurs around the cutout. Brogan and Almroth [13], Almroth and Holmes [14], and Almroth et al. [15] analyzed the effect of the cutouts on the elastic axial buckling strength with the finite difference code STAGS.

The effects of a circular hole on the elastic axial buckling strength and the local buckling behavior of a cylindrical shell were studied by Tennyson [16], Starnes [17], and Rahimi [18] respectively. An approximate lower bound to the limit load and torque of cylindrical shells with a single circular cutout was obtained by Foo [19].

Shu [20], Robert [21] investigated the limit load of cylindrical shells with circumferential cracks. Yun-Jae [22] provides approximate J estimates for off-centered, circumferential through-wall cracks in cylinders under bending.

Meng-kao [23] investigated the buckling behavior of an elasto plastic cylindrical shell with a cutout. Rahimi [24] have done a parametric study of plastic strength of cylindrical shells with cutout under bending moment and axial loading, also Rahimi [25] investigated the plastic analysis of cylindrical shells with a single circle cutout under bending moment with analytical method. However, to our knowledge the plastic analysis of a cylindrical shell with a cutout under pure bending, which is important in the design of aircraft and missile structures, little work were previously reported.

In this work, we considered an elastoplastic material and use finite element code, ABAQUS Software to analyze the plastic behavior of cylindrical shells with cutouts under pure bending. The shell had a circular cross section and both ends were clamped. The shape of the cutouts in the shell was circular or rectangular. The influence of the size, location and number of the cutouts on the limiting bending moment of a cylindrical shell is presented. The numerical results are compared with experimental ones for stainless steel tubes with ratios of diameter to thickness 40.4 and the length to diameter 7.94. The deformation during loading, the axial and circumferential stress

distribution around the cutouts of a cylindrical shell under bending is investigated.

2. EXPERIMENTS

The aim of the experiments was to determine bending moment collapse load of all specimens and stress distribution in circumferential and longitudinal direction around cutout of two specimens with square and circle cutouts. The experimental results are also used to verify the finite element results.

Measurement of material properties: Five strip specimens according to ASTM E8 standard (Tensile Tests) were cut from a tube to find the material specifications (E, ν, σ_y and σ_u). Tests have been carried out by Zwick Z100 apparatus with 10 tons capacity. The results are given in Table 1. Hereafter, we refer to these data as the ASTM tests.

Table 1. Material characteristics shell tested

Test Specimens	E (GPa)	σ_y (MPa)	σ_u (MPa)	ν
T1	188.30	351.26	706.51	
T2	187.15	343.26	697.74	
T3	195.12	342.79	703.06	
T4	182.2	419.19	708.98	
T5	188.17	364.12	715.12	0.297

Inorder to find the Poisson ratio, two strain gauges in the longitudinal and transverse direction was applied at inner and outer surfaces of T5 to measure the longitudinal and transverse strains (Figure 1). After recording the strains in two directions, the Poisson ratio is obtained as 0.297. It is seen that, the calculated Poisson ratio is approximately equal to the values recorded in the handbooks.

Figure 1. Tensile test T5 (strain gauges and extensometer)

For calibrating the strain gauges, length variation of T5 specimen is measured with extensometers and compared with values of longitudinal strain gauge measurement.

Specimens: 17 specimens, called M6 to M21 were designed and provided from tubes with 62mm diameter and 1.5mm thickness (Figure 2). The tubes were made from stainless steel 304, rolled and seam welded along a longitudinal line.

Figure 2. Tube specimens

The tested specimens were provided with specification in Table 2 and categorized into five dissimilar groups. In group 1 the effect of size of circle cutout, in groups 2,3 the position and numbers of the circle cutouts, in groups 4,5 the size of length and width size of quadrilateral cutout on the plastic moment were investigated. In groups 1,4 and 5, center of the cutout were produced diametrically opposite of the seam-welded line. In-group 2 the position of cutout is varied in circumferential direction with interval 90° and in-group 3 the numbers of cutout are varied.

Measurement devices: Two set universal machine with 10 and 60 tons capacity, strain gauges, data acquisition system and pure bending measurement device.

Data acquisition system included: a computer (Pentium 4, Intel 1.7GHZ), PCI 1710 HG card (Advantech) with eight differential channels and Lab View software.

Strain gauges with thermal compensation between -45°C to +95°C for precision static transducer service, type EA-I3-T034R-350, M&M, with R=(350+0.15%) OHM

Chemical and dimension analysis (gauge length, thickness, Radius and length) over the tensile tests and tubes (two cylindrical specimens) were done and material was obtained stainless steel 304 as expected.

A testing device (pure bending measurement), approximately similar to that made by

Gibson [26], was designed and made to perform experiments on bending moment tests (Figure 3).

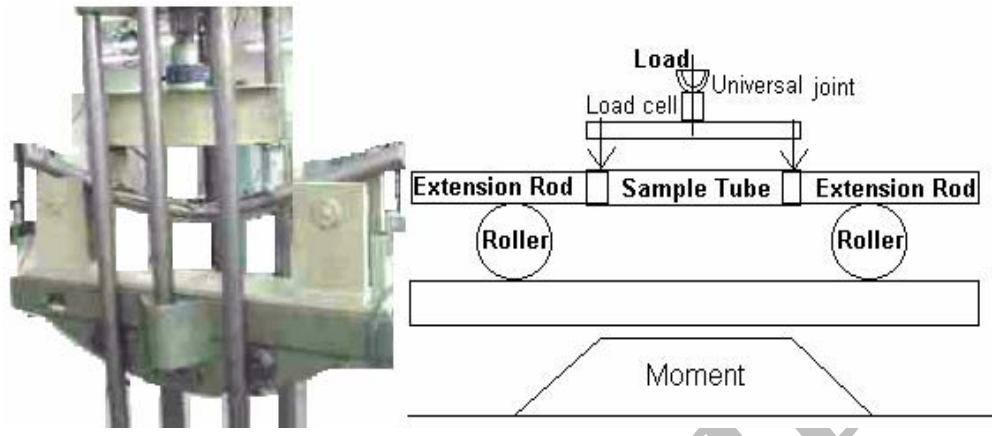

Figure 3. Schematic of bending test machine

Table 2. Specification of specimens

Mark	Number of cutout	Number of strain gauges	Position of cutout [degrees]	Dimension of cutout [mm]	Type of cutout
M6	0	-	-	-	-
M7	1	-	0	r=3.0	Circular
M8	1	-	0	r=7.5	Circular
M9	1	-	0	r=15.0	Circular
M10	1	-	180	r=7.5	Circular
M11	1	-	90	r=7.5	Circular
M12	1	8	0	r=7.5	Circular
M13	2	-	0, 180	r=7.5	Circular
M14	3	-	0, 120, 240	r=7.5	Circular
M15	4	-	0, 90, 180, 270	r=7.5	Circular
M16	1	-	0	a=16.5, b=1.5	Rectangular
M17	1	-	0	a=6 , b=15	Rectangular
M18a	1	-	0	a=15, b=15	Square
M18b	1	8	0	a=15, b=15	Square
M19	1	-	0	a=15, b=30	Rectangula

					r
M20	1	-	0	a=30, b=15	Rectangular
M21	1	-	0	a=30, b=30	Square

For testing, a set of extension rods was used for both ends of each specimen. A universal machine, AMSLER type SZBDA with 60-tons capacity was used to apply axial load over the extension rods and to rotate them to produce pure bending on specimens. A load cell connected to the beam was used to measure the force. Two electrical displacement transducers and two-dial gauge were used to measure the displacements and rotations of ends and two another points of specimens. The signals of the displacement transducers, strain gauges and load cell were amplified and fed into a data acquisition card built into a computer to obtain the relationship between the bending moment and the total end rotation of the specimen.

Typical experimental results of specimens group 1 with circle cutout (diameter varied from zero to 15mm) on the compression side at the middle length are shown in Figure 4. Since the bending rigidity of the shell with a cutout is not uniform along the shell axis, the total end rotation of the shell is used as the abscissa. The circular and rectangular cutouts affected both the limiting buckling moment and post buckling behavior of the moment – rotation response.

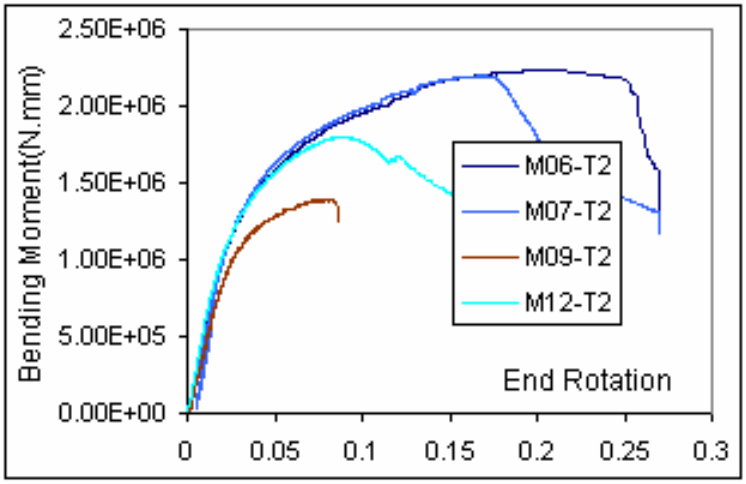

Figure 4. Experimental moment-end rotation responses of cylindrical shell under bending moment (Group 1)

In two specimens, M12and M18b, additional instrumentation consisted of elements resistance foil strain gauges and mechanical dial gauges were used to observe displacements. Strain measurements were concentrated around the cutout, with emphasis on the edges and around the central and end circumferences of the cutouts. The strain gauges were mounted parallel to the longitudinal axis in points 2,4,5,7,9 and circumferential axis in point 1,3,6,8.

A typical arrangement of strain gauges is shown in Figure 5.

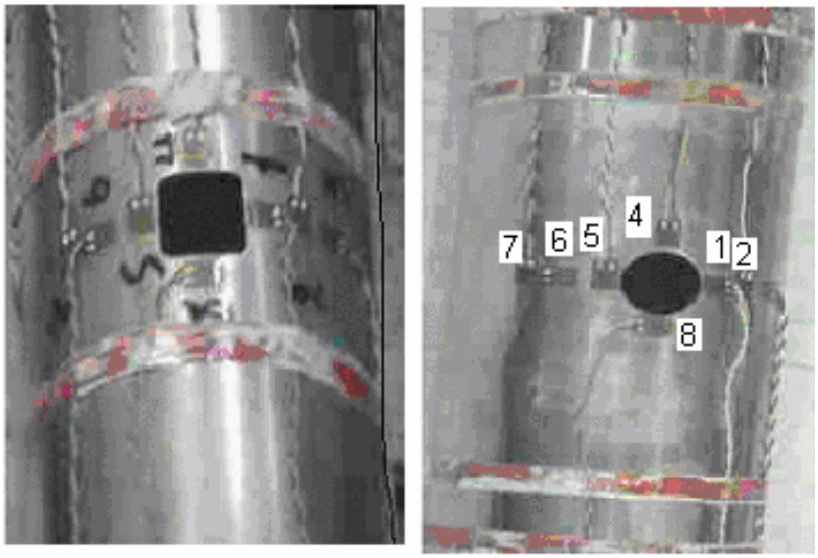

Figure 5. Strain gauges layout for specimens M12 and M18b

3. FINITE ELEMENT MODEL

Seventeen asymmetric finite element models in order to validate experimental results and to extend the analysis to other geometries and loading conditions. The ABAQUS [27] software package was employed. The program can perform both material and geometry nonlinear analysis with extensive options for element selection. A schematic with model dimensions is depicted in Figure 5.

Element and Mesh Discretization: In ABAQUS isoparametric RIP shell elements are used, which appears to be good approach for nonlinear cases. The elements are a single type S8R5, 8-node isoparametric, reduced integration shell element. The number of integration points of an element is 4.

Since the cutout presents a sudden discontinuity in geometry and thereby very high stresses expected near the hole which is decay within a small zone away from the cutout, it is necessary to use relatively small elements in the region close to the opening in order to monitor these high stresses and their gradients. The element mesh may become coarser away from this region. The finial mesh resulted from a ‘convergence study’ consisted of 3532 elements and illustrated in Figure 6.

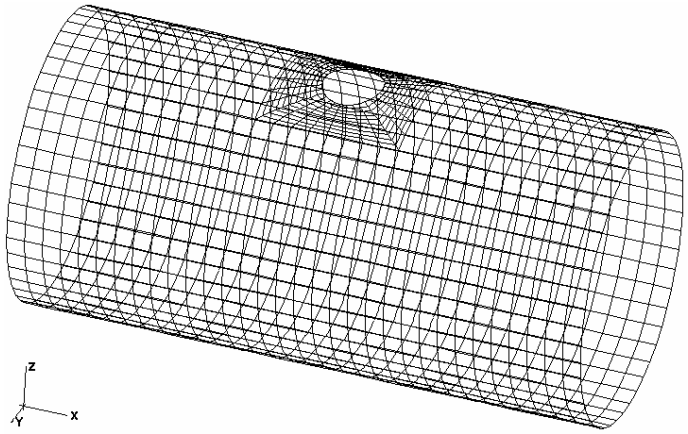

Figure 6. Mesh configureuration

Kinematics Boundary Conditions: The boundary conditions considered here were naturally displacements. One point at opposite side of hole is fixed, and all degrees of freedom are imposed to be zero.

The kinematics boundary condition to be imposed is at the end planes where the bending moment is applied. Beam nodes are introduced to represent the motion of the end planes. The end sections may be treated as rigidly attached to stiff plates, as appears to be the case in the analysis. The kinematics conditions at the end planes are thus: (a) the shell nodes must remain in the plane after deformation, (b) there can be no rotation about the X and Z axes, (c) the component of rotation about the Y axis must be the same for each shell node on the end planes as that the beam node, and (d) the circular cross section of the end planes remains circular after deformation.

They are not simple boundary conditions, but are multi-point constraints (MPC's), because they involve equations between several degrees of freedom in the model. A user subroutine was written to impose the above boundary conditions.

Loading: For bending moment the ABAQUS suite requires the rotation value applied at the end plane to beam node. Prior to the plastic analysis, an elastic analysis was required, in order to determine the approximate value of the rotation to be applied at the end flange. The increment of rotation at the end nodes is applied in steps and the resulting moment required to produce this rotation is obtained by given reactions at the beam node.

4. DISCUSSION OF RESULTS

4.1. Bending moment

Figure 7 Shows numerical and experimental bending moment-end rotation behavior of specimen M12 with circle cutout typically. The behavior of moment-end rotation curves in the elastic range is similar experimentally and numerically, but there are differences in the plastic range in almost all the specimens.

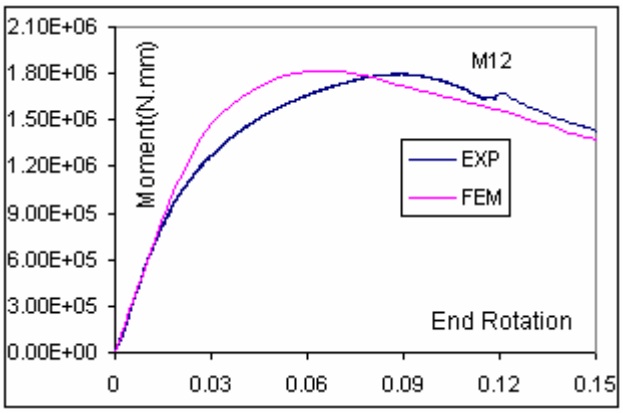

Figure 7. Numerical and experimental bending moment-end rotation behavior of specimen M12

The influence of the size of cutout on the limit moment of shells with a circular cutout is shown in Figure 8. Cutout was located at the middle of the compression side of the shells. The limiting bending moment M_b and the diameter of the cutout d, were made dimensionless by the perfect plastic moment of a perfect cylindrical shell M_p defined in the following equation, and the shell radius R, respectively.

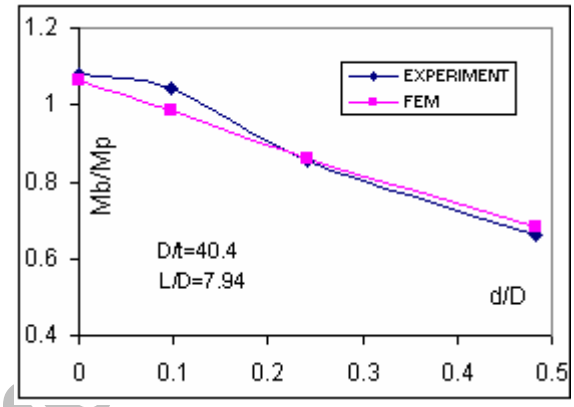

Figure 8. Effect of circle cutout size on the limiting buckling moment of cylindrical shells

$$M_P = 4R^2 t\sigma_y \quad (1)$$

in which σ_y is the yield stress of the material.

The limiting buckling moment M_b obviously decreased as the diameter of the circular cutout increased. The end rotation at buckling θ_b decreased as the dimensionless diameter of the circular cutout increased from 0 to 0.484. The influence of the size of cutout on the limiting buckling moment of shells with a rectangular cutout is shown in Figure 9

experimentally. The abscissa is expressed by the ratio b/D, a/D for shells of diameter D=62 mm. The results expressed as two line show that the longitudinal length b of the rectangular cutout increased from 1.5 mm to 30 mm when a=15 mm and the other line show that the circumferential length a of the rectangular cutout increased from 6 mm to 30 mm when b=15 mm. The limiting buckling moment decreased as the size of the rectangular cutout increased. Increasing a, the length in circumferential direction, has a stronger influence on the limiting buckling moment.

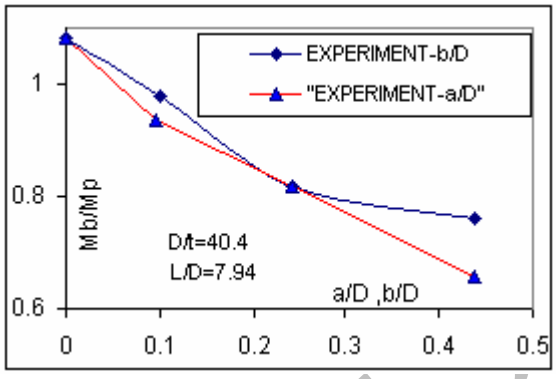

Figure 9. Effect of square cutout size on the limiting buckling moment of cylindrical shells

The location of the circular cutout (a = 15 mm) along the circumference has an effect on the limiting buckling moment of the shell as shown in Figure 10. As the circular cutout moved from the compression side (ϕ=0) to the tension side (ϕ=180) of the shell, the limiting buckling moment increased first from ϕ=0 to ϕ=90; then the limiting buckling moment is approximately constant from ϕ=90 to ϕ=180. According to Figure. 10, shells with a cutout on the compression side have smaller limiting buckling moments than those with a cutout on the tension side.

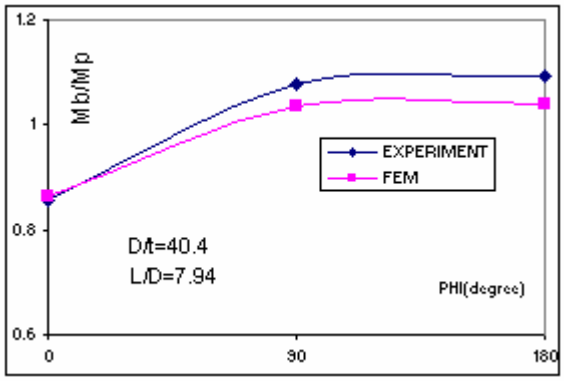

Figure 10. Effect of cutout position on the limiting buckling moment of cylindrical shells

The limiting buckling moment of shells with 1,2,3 and 4 circular cutouts (d=15 mm) is shown in Figure 11. As the cutout number is increased from 1 to 2 or 3, the limiting buckling moment remained almost constant.

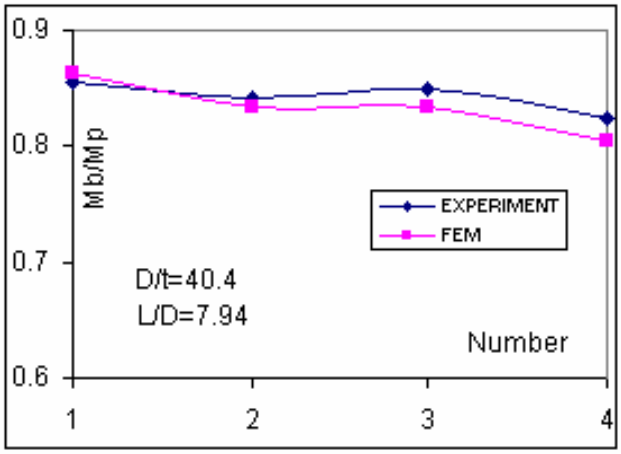

Figure 11. Effect of number of cutout on the limiting buckling moment of cylindrical shells

4.2. Strain distribution

Figure 12 shows numerical and experimental results for longitudinal ε_L and circumferential ε_C components of the strain field around of cutout, in the outer surface of the specimen M12 under bending moment plastic load.

In the analytical viewpoint, point 9 (SN9) is on the position of the neutral axis. This has been obtained by numerical and experimental analysis results, so that the strain value of point 9 from zero loads until vicinity of collapse load is negligible. But after collapse, due to instability, the above area exposed to compressive strain (Figure 12-a)

From the viewpoint of strain behavior, experimental and numerical analysis findings are in a good agreement at point 5 until collapse load, but approximately in around of it. This difference increases due to the existence instability, by the way their behavior are similar to each other (Figure 12-b).

The experimental results related to longitudinal and circumferential strain distribution in the around of cutout are a good agreements with numerical analysis. Therefore, it can be used to presented FEM for determining of strain distribution in inner, middle and outer surfaces of the cylindrical shell. The distribution of strain around of square cutout of specimen M18b was shown to be similar to M12 specimen by using of numerical and experimental methods.

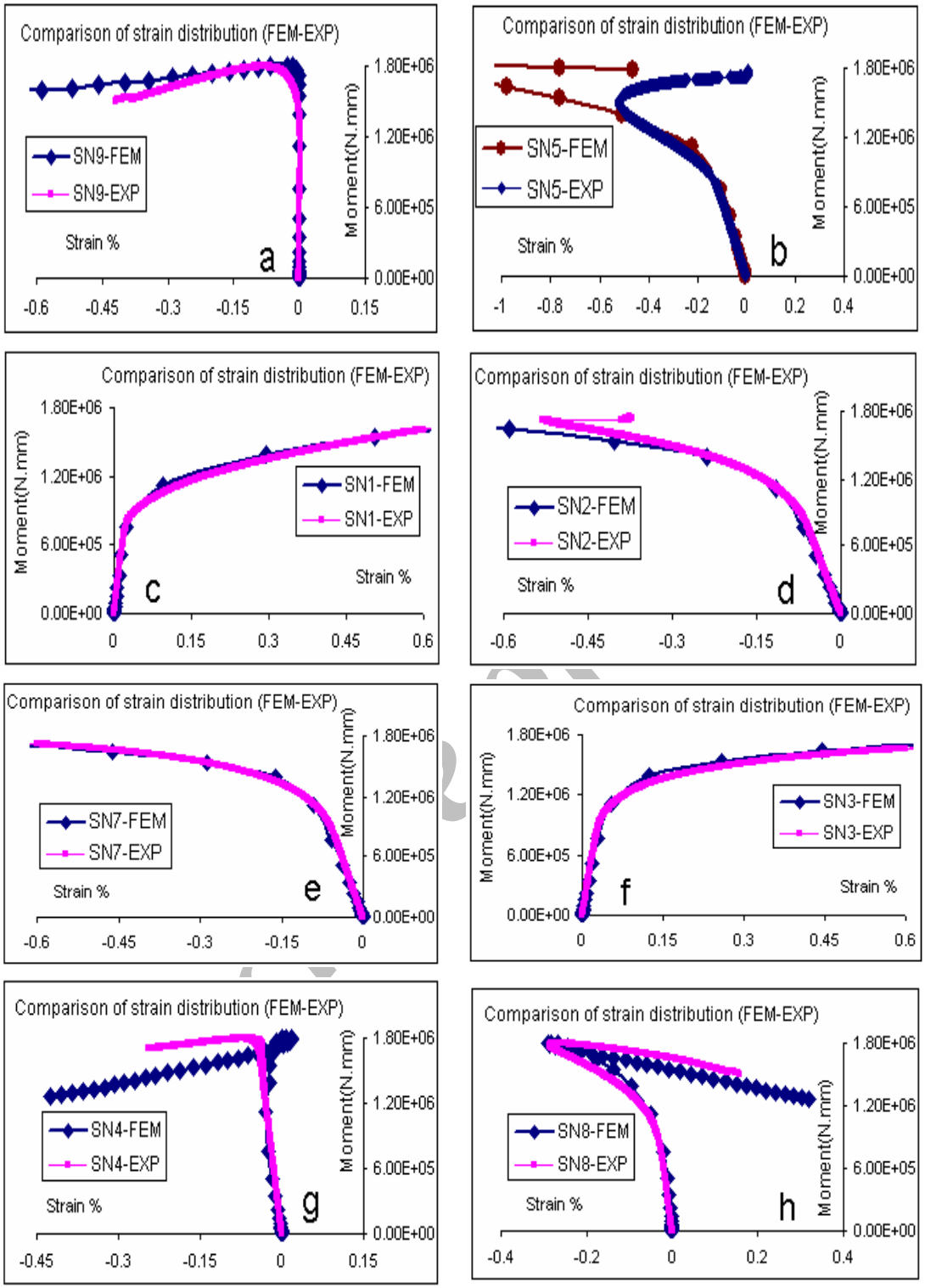

Figure 12. Strain distribution around cutout of cylindrical shell under bending moment

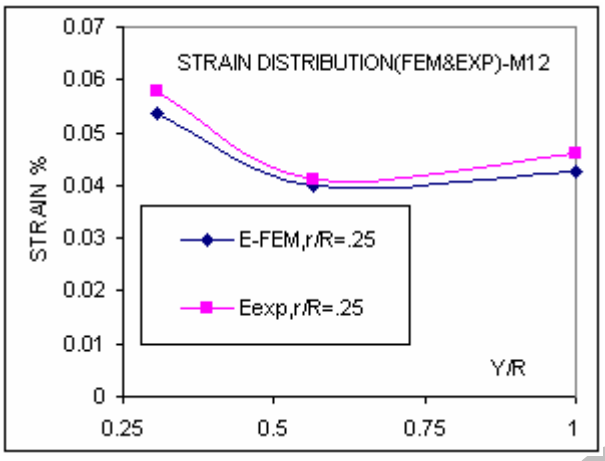

Figure 13. Comparison of strain results (Circular Cutout)

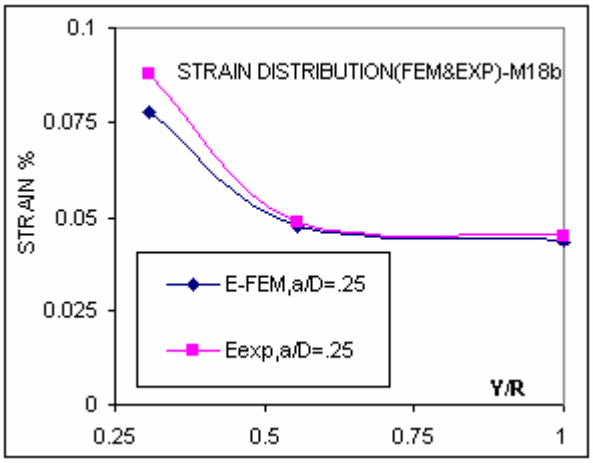

Figure 14. Comparison of strain results (square cutout)

Figures 13 and 14 show that the numerical and experimental results for longitudinal stress around of cutout, in the outer surface of the specimens M12 & M18b under axial elastic load have good agreement. Therefore it can be concluded that the longitudinal and circumferential strain values decrease with increasing of distance from the cutout edge.

So, longitudinal stress concentration factor from edge of hole until 90 degree in the circumferential direction in cylindrical shells with different radius of two kinds of cutouts are calculated with FEM (Figures 15 and 16).

Results show that stress concentration factor increases with increasing sizes of cutouts and also stress value decreases in the area far from of hole.

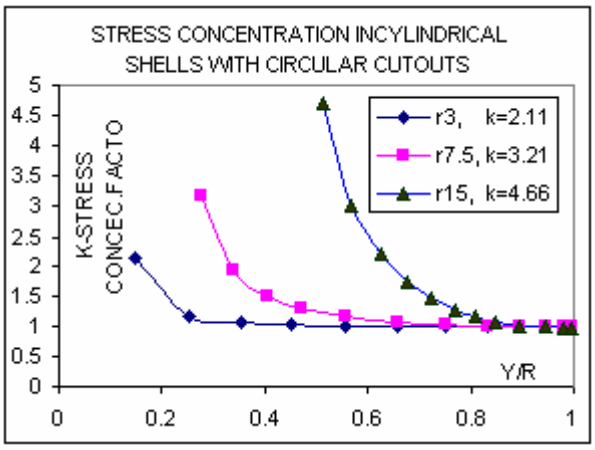

Figure 15. Longitudinal stress distribution along circumferential direction in cylindrical shells with different radius circle cutout

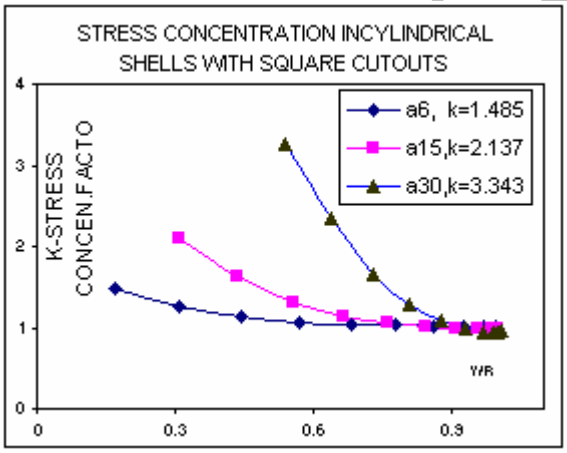

Figure 16. Longitudinal stress distribution along circumferential direction in cylindrical shells with different length square cutout

5. CONCLUSIONS

The elastoplastic buckling of cylindrical shells of circular cross section with a cutout under pure bending was investigated analytically and experimentally. A bending test facility was established to perform the pure bending buckling experiments. The bending buckling and post-buckling behavior of the circular cylindrical shells with a circular or rectangular cutout were observed. Similar results were also obtained from finite element analyses in which an incremental displacement- controlled scheme was developed to ensure the pure bending condition. For the cases studied, we draw the following conclusions:

- The existence of a cutout altered the nature of the moment–end rotation response and diminished the limiting buckling moment of a cylindrical shell under pure bending.
- For a shell with a circular cutout, the limiting buckling moment was decreased on increasing diameter of the cutout; for a shell with a rectangular cutout, the limiting buckling moment was decreased on increasing the size of the cutout.
- The limiting buckling moment of a shell with a cutout on the compression side is smaller than for the case of a cutout on the tension side.
- The limiting buckling moment of a shell with a cutout increased when the cutout was located toward one end of the clamped shell.
- A comparative analysis of local strains obtained numerically and experimentally in the elasto-plastic deformation range shows a good coincidence in a character of corresponding dependences but reveals some difference in the maximum elastic strain values resulting from two approaches concerned. This little difference makes itself most evident in a high strain gradient zone and increases with the growth of applied load level and also this difference is due to nonlinearity in primary loading in experimental tests.
- The results of experimental and numerical analysis show that stress concentration in edge of both kinds of cutouts is increased but it in circular cutout is more than in square cutouts. Stress distribution decreases form edge of the hole in circumferential direction until a distance of hole, then stress value is fixed and closed to stress calculated with theoretical analysis in a cylindrical shell without any defect
- Maximum stress concentration in a thin plane specimen with a hole under tension is equal to three. Comparison of the stress concentration results of cylindrical shells with small size cutouts shows that the stress concentration of thin plane more than of cylindrical shell with square cutouts and less than of cylindrical shell with circular cutouts.
- One of the applications of this study is to make the first step to define stress distribution on the cylindrical shells with cutouts under cyclic in service loading. Stress or strain concentration as the main reason for the occurrence of local elastic or elasto - plastic strains. This leads to a decrease in the structures lifetime in accordance with low cycle fatigue laws.

Acknowledgement: The authors would like to express appreciation to their colleagues in the Laboratory of Mechanical Engineering Department of Sharif University for preparing the experimental facilities.

REFERENCES

1. Brazier LG. On the flexure of thin cylindrical shells and other section. *Proc R. Soc. Lond*., **A116**(1927)104–114.
2. Seide P, Weingarten VI. On the buckling of circular cylindrical shells under pure bending. *ASME J. Appl Mech*, **28**(1961) 112–116.
3. Sherman DR. Tests of circular steel tubes in bending. *ASCE J. Struct Div*.,

102(1976)2181-95.
4. Reddy BD. An experimental study of the plastic buckling of circular cylinders in pure bending. *Int. J. Solids Struct*, **15**(1979) 669-683.
5. Tugcu P, Schroeder J. Plastic deformation and stability of pipes exposed to external couples. *Int. J. Solids Struct*, **15**(1979) 643-658.
6. Gellin S. The plastic buckling of long cylindrical shell under pure bending. *Int. J. Solids Struct*, **16**(1980) 397-407.
7. Bushnell D. Elastic–plastic bending and buckling of pipes and elbows. *Int. J. Comput Struct*, **13**(1981) 241-248.
8. Kyriakides S, Ju GT. Bifurcation and localization instabilities in cylindrical shells under bending. I. Experiments. *Int J. Solids Struct*, **29**(1992) 1117-1142.
9. Ju GT, Kyriakides S. Bifurcation and localization instabilities in cylindrical shells under bending. II. Predictions. *Int J. Solids Struct*, **29**(1992) 1143-1171.
10. Corona E, Kyriakides S. An unusual mode of collapse of tubes under combined bending and pressure. *ASME J. Press Vessel Technology,* **109**(1987) 302-304.
11. Shaw PK, Kyriakides S. Inelastic analysis of thin-walled tubes under cyclic bending. *Int J. Solids Struct*., **21**(1985) 1073-1100.
12. Shaw PK, Kyriakides S. Inelastic buckling of tubes under cyclic bending. *ASME J Press Vessel Technology*, **109**(1987) 169-178.
13. Brogan F, Almroth BO. Buckling of cylinders with cutouts. *AIAA J.*, **8**(1970) 236-240.
14. Almroth BO, and Holmes AMC. Buckling of shells with cutouts, experiment and analysis. *Int J Solids Struct*, **8**(1972) 1057-1071.
15. Almroth BO, Brogan F, and Marlowe MB. Stability analysis of cylinders with circular cutouts. *AIAA J*., **11**(1973) 1582-1584.
16. Tennyson RC. The effects of unreinforced cutouts on the buck-ling of circular cylindrical shells under axial compression. *ASME J Eng Ind*, **90**(1968) 541-546.
17. Starnes JH. Effects of a circular hole on the buckling of cylindrical shells loaded by axial compression. *AIAA J*., **10**(1972) 1466-1472.
18. Rahimi G. H. and Nobahari G.R. Parametric Study of Elastic Buckling of Cylindrical Shells with Cutout under Axial Loading. *J. Mech. Eng. Soc. of Iran,* **4**(2001) 31-58(in Persian language)
19. Foo, S S B. On the limit analysis of cylindrical shells with a single cutout. *Int. J. Press. Ves. and Piping*, **49**(1992) 1-16.
20. Shu Hengmu. The plastic limit load of circumferentially cracked thin walled pipes under axial force. *International Pressure and Asymmetrical Bending*, **79**(2002) 377-382.
21. Robert, F. and Rahman, S. Elastic-Plastic analysis of off-center cracks in cylindrical structures. *Engineering fracture mechanics*, **66**(2000) 15-39.
22. Yun-Jae Km, Do-Jun Shim. Approximate elastic-plastic J estimates of cylinders through wall cracks. *Engineering Fracture Mechanic*. **71**(2004) 1673-1693.
23. Meng-Kao Yeh, Meng-Chyuan Lin, and Wen-Tsang Wu. Bending Buckling of an Elasto-plastic Cylindrical Shell with a Cutout. *Engineering Structures*, **21**(1999) 996-1005.

24. Rahimi G H, and Poursaeidi E. Parametric study of plastic strength of cylindrical shells with cutout under bending moment and axial loading. *J. Mech. Eng. Soc. of Iran*. 2004 (in Persian language).
25. Rahimi G H, and Poursaeid. E. Plastic analysis of cylindrical shells with a single cutout under bending moment. *The 3rd international conference on advances in structural engineering and Materials*, 2-4 September 2004, Seoul, Korea.
26. Karam, G.N. and Gibson, L.J. Elastic buckling of cylindrical shells with elastic cores-II Experiments. *Int. J. solids structures*, **89**(1995) 1285-1306.
27. ABAQUS FEA Version 5.7-5. Hibbit, Karlsson and Sorensen, Inc. 1998.